

# Novel Density-Wave States of Two-Band Peierls-Hubbard Chains

Shoji Yamamoto

*Department of Physics, Faculty of Science, Okayama University,  
Tsushima, Okayama 700-8530, Japan*

(Received 11 May 1998)

Based on a symmetry argument we systematically reveal Hartree-Fock broken-symmetry solutions of the one-dimensional two-band extended Peierls-Hubbard model, which covers various materials of interest such as halogen-bridged metal complexes and mixed-stack charge-transfer salts. We find out all the regular-density-wave solutions with an ordering vector  $q = 0$  or  $q = \pi$ . Changing band filling as well as electron-electron and electron-phonon interactions, we numerically inquire further into the ground-state phase diagram and the physical property of each state. The possibility of novel density-wave states appearing is argued.

## I. INTRODUCTION

One-dimensional two-band models with competing electron-electron (el-el) and electron-phonon (el-ph) interactions have been attracting considerable interest. Such models cover quasi-one-dimensional materials such as halogen-bridged transition-metal (MX) linear-chain complexes and charge-transfer (CT) salts with mixed-stacks of alternating donor and acceptor molecules. They are also one-dimensional analogs [1] of the multiband models for  $\text{CuO}_2$  planes in high-temperature superconductors. We retain electronic orbitals of different kinds in our calculation not only due to a quantitative explanation of experiments but also because we are fascinated by the models themselves which could bring us unusual phenomena beyond the single-band description [2,3]. One of the most interesting consequences of intrinsic multi-band effects and the competition between el-el and el-ph interactions may be the variety of ground states. Employing a group-theoretical technique the present author and Ozaki [4,5] studied the three-band Peierls-Hubbard model on a square lattice and obtained plenty of novel broken symmetry phases. Gammel *et al.* [6] investigated a similar model but with both site-diagonal and site-off-diagonal el-ph interactions. Besides regular-density-wave states [7], they pointed out several novel solutions such as incommensurate long-period phases [8] and a spin-frustrated state [9].

Some of the ground states predicted above were observed experimentally. Charge-transfer compounds with mixed stacks such as TTF-chloranil [10] and  $\text{TTeC}_1\text{TTF-TCNQ}$  [11] may be described by a half-filled two-band

model with site-off-diagonal el-ph coupling. They are dimerized into bond-order-wave (BOW) states at low temperatures, which is recognized as a charge-transfer-induced spin-Peierls transition. Halogen-bridged metal complexes, which may be described by a 3/4-filled two-band model with site-diagonal el-ph coupling, exhibit a strong dependence of their ground states on the constituent metal and halogen ions. Familiar compounds of Pt ions [12] have the ground state with a charge density wave (CDW) on the metal sites induced by a dimerization of the halogen-ion sublattice, whereas recently synthesized Ni compounds [13,14] show a regular-chain structure with a spin density wave (SDW) on the metal sites. Although the interchain hydrogen-bond networks are not negligible here, the competition between the CDW and SDW states may be recognized as a crossover between the Peierls and Mott insulators. Thus observed rich phase diagrams allow us to expect further ground states unrevealed. Hence we here present a systematic Hartree-Fock (HF) study on competing broken-symmetry ground states. We focus on one dimension where ground-state properties could be most fascinating due to significant quantum effects. Based on a symmetry argument, we reveal possible ground states of regular-density-wave type and clarify their physical properties.

## II. MODEL HAMILTONIAN AND ITS SYMMETRY PROPERTY

We study the one-dimensional two-band extended Peierls-Hubbard model:

$$\begin{aligned} \mathcal{H} = & \sum_{n=1}^L \sum_{s=\pm} [\varepsilon_M - \beta(u_n - u_{n-1})] a_{1:n,s}^\dagger a_{1:n,s} + \sum_{n=1}^L \sum_{s=\pm} \varepsilon_X a_{2:n,s}^\dagger a_{2:n,s} \\ & - \sum_{n=1}^L \sum_{s=\pm} \left[ (t - \alpha u_n) a_{1:n,s}^\dagger a_{2:n,s} + (t + \alpha u_{n-1}) a_{1:n,s}^\dagger a_{2:n-1,s} + \text{H.c.} \right] \\ & + U_M \sum_{n=1}^L a_{1:n,+}^\dagger a_{1:n,+} a_{1:n,-}^\dagger a_{1:n,-} + U_X \sum_{n=1}^L a_{2:n,+}^\dagger a_{2:n,+} a_{2:n,-}^\dagger a_{2:n,-} \end{aligned}$$

$$+ V \sum_{n=1}^L \sum_{s,s'=\pm} \left[ a_{1:n,s}^\dagger a_{1:n,s} a_{2:n,s'}^\dagger a_{2:n,s'} + a_{1:n,s}^\dagger a_{1:n,s} a_{2:n-1,s'}^\dagger a_{2:n-1,s'} \right] + \frac{K}{2} \sum_{n=1}^L u_n^2. \quad (2.1)$$

Here we assume the Hamiltonian to describe MX chains. Now the Hamiltonian (2.1) is recognized as follows:  $a_{1:n,s}^\dagger$  and  $a_{2:n,s}^\dagger$  are the creation operators of an electron with spin  $s = \pm$  (up and down respectively) in the metal  $d_{z^2}$  and halogen  $p_z$  orbitals at unit cell  $n$ , respectively,  $u_n$  the chain-direction displacement from the uniform lattice spacing of the halogen atom at unit cell  $n$ , and  $L$  the number of unit cells composed of a pair of neighboring metal and halogen atoms;  $\varepsilon_M$  and  $\varepsilon_X$  are the energies of the metal  $d_{z^2}$  and halogen  $p_z$  orbitals on isolated atoms, respectively,  $t$  the transfer energy of hopping between these levels,  $U_M$ ,  $U_X$ , and  $V$  the el-el interactions on the metal atoms, on the halogen atoms, and between the neighboring metal and halogen atoms, respectively;  $\alpha$ ,  $\beta$ , and  $K$  denote the site-off-diagonal and site-diagonal el-ph coupling constants and the elastic constant, respec-

tively. We stress that the model essentially covers various materials. For example, replacing the  $d_{z^2}$  and  $p_z$  orbitals by  $p\pi$  orbitals of donor and acceptor molecules, respectively, we can immediately switch our argument to organic mixed-stack CT compounds. Fourier transforms

$$\begin{aligned} a_{1:n,s}^\dagger &= \frac{1}{\sqrt{L}} \sum_k e^{-ikn} a_{1:k,s}, \\ a_{2:n,s}^\dagger &= \frac{1}{\sqrt{L}} \sum_k e^{-ik(n+1/2)} a_{2:k,s}, \\ u_n &= \frac{1}{\sqrt{L}} \sum_k e^{-ik(n+1/2)} u_k, \end{aligned} \quad (2.2)$$

compactly rewrite the Hamiltonian as

$$\begin{aligned} \mathcal{H} &= \sum_{i,j} \sum_{k,q} \sum_{s,s'} \langle i : k + q, s | t | j : k, s' \rangle a_{i:k+q,s}^\dagger a_{j:k,s'} \\ &+ \frac{1}{2} \sum_{i,j,m,n} \sum_{k,k',q} \sum_{s,s',t,t'} \langle i : k + q, s; m : k', t | v | j : k, s'; n : k' + q, t' \rangle \\ &\times a_{i:k+q,s}^\dagger a_{m:k',t}^\dagger a_{n:k'+q,t'} a_{j:k,s'}, + \frac{K}{2} \sum_k u_k u_k^*, \end{aligned} \quad (2.3)$$

where

$$\langle i : k + q, s | t | j : k, s' \rangle = \langle i : k + q | t | j : k \rangle \delta_{ss'}, \quad (2.4)$$

$$\begin{aligned} \langle i : k + q, s; m : k', t | v | j : k, s'; n : k' + q, t' \rangle \\ = \langle i : k + q; m : k' | v | j : k; n : k' + q \rangle \delta_{ss'} \delta_{tt'}, \end{aligned} \quad (2.5)$$

are specified as

$$\begin{aligned} \langle 1 : k + q | t | 1 : k \rangle &= \tilde{\varepsilon}_M \delta_{q0} - \frac{2i\beta}{\sqrt{L}} u_q^* \sin\left(\frac{q}{2}\right), \\ \langle 2 : k + q | t | 2 : k \rangle &= \tilde{\varepsilon}_X \delta_{q0}, \\ \langle 1 : k + q | t | 2 : k \rangle &= -2t_0 \cos\left(\frac{k}{2}\right) \delta_{q0} \\ &+ \frac{2i\alpha}{\sqrt{L}} u_q^* \sin\left(\frac{k+q}{2}\right), \quad (2.6) \\ \langle 1 : k + q; 1 : k' | v | 1 : k; 1 : k' + q \rangle &= \frac{U_M}{L}, \\ \langle 2 : k + q; 2 : k' | v | 2 : k; 2 : k' + q \rangle &= \frac{U_X}{L}, \\ \langle 1 : k + q; 2 : k' | v | 1 : k; 2 : k' + q \rangle &= \frac{2V}{L} \cos\left(\frac{q}{2}\right). \quad (2.7) \end{aligned}$$

with the renormalized on-site affinities  $\tilde{\varepsilon}_M = \varepsilon_M - U_M/2$  and  $\tilde{\varepsilon}_X = \varepsilon_X - U_X/2$ .

The symmetry group of the system is generally represented as

$$\mathbf{G} = \mathbf{P} \times \mathbf{S} \times \mathbf{T}, \quad (2.8)$$

where  $\mathbf{P} = \mathbf{L}_1 \wedge \mathbf{C}_2$  is the space group of a linear chain with the one-dimensional translation group  $\mathbf{L}_1$  whose basis vector is the unit-cell translation  $l_1$ ,  $\mathbf{S}$  the group of spin-rotation, and  $\mathbf{T}$  the group of time reversal. We here take no account of the gauge group because we do not consider superconducting phases. Group actions on the creation operators are defined as follows [15,16]:

$$l \cdot a_{i:k,s}^\dagger = e^{-ikl} a_{i:k,s}^\dagger, \quad (2.9)$$

$$p \cdot a_{i:k,s}^\dagger = a_{i:pk,s}^\dagger, \quad (2.10)$$

$$u(\mathbf{e}, \theta) \cdot a_{i:k,s}^\dagger = \sum_{s'} [u(\mathbf{e}, \theta)]_{ss'} a_{i:k,s'}^\dagger, \quad (2.11)$$

$$t \cdot (f a_{i:k,s}^\dagger) = -s f^* a_{i:-k,-s}^\dagger, \quad (2.12)$$

where  $l \in \mathbf{L}_1$ ,  $p \in \mathbf{C}_2$ ,  $u(\mathbf{e}, \theta) \in \mathbf{S}$ ,  $t \in \mathbf{T}$ , and  $f$  is an arbitrary complex number.  $u(\mathbf{e}, \theta) = \sigma^0 \cos(\theta/2) - (\boldsymbol{\sigma} \cdot \mathbf{e}) \sin(\theta/2)$  represents the spin rotation of angle  $\theta$  around an axis  $\mathbf{e}$ , where  $\sigma^0$  is the  $2 \times 2$  unit matrix and  $\boldsymbol{\sigma} = (\sigma^x, \sigma^y, \sigma^z)$  is a vector composed of the Pauli matrices.

Let  $\check{G}$  denote the irreducible representations of  $\mathbf{G}$  over the real number field, where their representation space is spanned by the Hermitian operators  $\{a_{i:k,s}^\dagger a_{j:k',s'}\}$ .

There is a one-to-one correspondence [17,18] between  $\check{G}$  and broken-symmetry phases with a definite ordering vector. Any representation  $\check{G}$  is obtained as a Kronecker product of the irreducible representations of  $\mathbf{P}$ ,  $\mathbf{S}$ , and  $\mathbf{T}$  over the real number field:

$$\check{G} = \check{P} \otimes \check{S} \otimes \check{T}. \quad (2.13)$$

$\check{P}$  is characterized by an ordering vector  $q$  in the Brillouin zone and an irreducible representation of its little group  $\mathbf{P}(q)$  [19], and is therefore labeled  $q\check{P}(q)$ . The relevant representations of  $\mathbf{S}$  and  $\mathbf{T}$  are, respectively, given by

$$\check{S}^0(u(\mathbf{e}, \theta)) = 1, \quad \check{S}^1(u(\mathbf{e}, \theta)) = O(u(\mathbf{e}, \theta)), \quad (2.14)$$

$$\check{T}^0(t) = 1, \quad \check{T}^1(t) = -1, \quad (2.15)$$

where  $O(u(\mathbf{e}, \theta))$  is the  $3 \times 3$  orthogonal matrix satisfying  $u(\mathbf{e}, \theta)\boldsymbol{\sigma}^\lambda u^\dagger(\mathbf{e}, \theta) = \sum_{\mu=x,y,z} [O(u(\mathbf{e}, \theta))]_{\lambda\mu} \boldsymbol{\sigma}^\mu$  ( $\lambda = x, y, z$ ). The representations  $\check{P} \otimes \check{S}^0 \otimes \check{T}^0$ ,  $\check{P} \otimes \check{S}^1 \otimes \check{T}^1$ ,  $\check{P} \otimes \check{S}^0 \otimes \check{T}^1$ , and  $\check{P} \otimes \check{S}^1 \otimes \check{T}^0$  correspond to charge-density-wave (CDW), spin-density-wave (SDW), charge-current-

wave (CCW), and spin-current-wave (SCW) states, respectively. We leave out current-wave states in our argument, because here in one dimension all of them but one-way uniform-current states break the charge- or spin-conservation law. The current states in one dimension are less interesting than in higher dimensions, where physically stimulative ones [4,15,16,20] may appear. We consider two ordering vectors  $q = 0$  and  $q = \pi$ , which are labeled  $\Gamma$  and  $X$ , respectively. Thus we treat the instabilities characterized as  $\Gamma\check{P}(\Gamma) \otimes \check{S}^0 \otimes \check{T}^0$ ,  $X\check{P}(X) \otimes \check{S}^0 \otimes \check{T}^0$ ,  $\Gamma\check{P}(\Gamma) \otimes \check{S}^1 \otimes \check{T}^1$ , and  $X\check{P}(X) \otimes \check{S}^1 \otimes \check{T}^1$ . Here  $\check{P}(\Gamma)$  and  $\check{P}(X)$  are either  $A$  ( $C_2$ -symmetric) or  $B$  ( $C_2$ -antisymmetric) representation of  $\mathbf{C}_2$  because  $\mathbf{P}(\Gamma) = \mathbf{P}(X) = \mathbf{C}_2$  in the present system.

### III. BROKEN SYMMETRY SOLUTIONS

In the HF approximation the Hamiltonian (2.3) is replaced by

$$\mathcal{H}_{\text{HF}} = \sum_{i,j} \sum_{k,s,s'} \sum_{\lambda=0,z} \left[ x_{ij}^\lambda(\Gamma; k) a_{i:k,s}^\dagger a_{j:k,s'} + x_{ij}^\lambda(X; k) a_{i:k+\pi,s}^\dagger a_{j:k,s'} \right] \sigma_{ss'}^\lambda, \quad (3.1)$$

where  $x_{ij}^\lambda(K; k)$  is the self-consistent renormalized field describing nonmagnetic ( $\lambda = 0$ ) and magnetic ( $\lambda = z$ ) instabilities at point  $K$  and is expressed as

$$\begin{aligned} x_{ij}^0(\Gamma; k) &= \langle i : k | t | j : k \rangle + \sum_{m,n} \sum_{k'} \rho_{nm}^0(\Gamma; k') \\ &\quad \times [2\langle i : k; m : k' | v | j : k; n : k' \rangle - \langle i : k; m : k' | v | n : k'; j : k \rangle], \\ x_{ij}^z(\Gamma; k) &= - \sum_{m,n} \sum_{k'} \rho_{nm}^z(\Gamma; k') \langle i : k; m : k' | v | n : k'; j : k \rangle \\ x_{ij}^0(X; k) &= \langle i : k + \pi | t | j : k \rangle + \sum_{m,n} \sum_{k'} (-1)^{\delta_{m2}} \rho_{nm}^0(\Gamma; k') \\ &\quad \times [2\langle i : k + \pi; m : k' | v | j : k; n : k' + \pi \rangle - \langle i : k + \pi; m : k' | v | n : k' + \pi; j : k \rangle], \\ x_{ij}^z(X; k) &= - \sum_{m,n} \sum_{k'} (-1)^{\delta_{m2}} \rho_{nm}^z(\Gamma; k') \langle i : k + \pi; m : k' | v | n : k' + \pi; j : k \rangle. \end{aligned} \quad (3.2)$$

Here we have introduced the density matrices

$$\begin{aligned} \rho_{ij}^\lambda(\Gamma; k) &= \frac{1}{2} \sum_{s,s'} \langle a_{j:k,s}^\dagger a_{i:k,s'} \rangle_{\text{HF}} \sigma_{ss'}^\lambda, \\ \rho_{ij}^\lambda(X; k) &= \frac{1}{2} \sum_{s,s'} \langle a_{j:k+\pi,s}^\dagger a_{i:k,s'} \rangle_{\text{HF}} \sigma_{ss'}^\lambda, \end{aligned} \quad (3.3)$$

where  $\langle \dots \rangle_{\text{HF}}$  denotes the quantum average in a HF eigenstate. We note that nonaxial magnetic instabilities ( $\lambda = x, y$ ) are not obtained from the Hamiltonian

$$\begin{aligned} h^0(\Gamma; A) &= \sum_{k,s} c_1^0(\Gamma; A) a_{1:k,s}^\dagger a_{1:k,s} + \sum_{k,s} c_2^0(\Gamma; A) a_{2:k,s}^\dagger a_{2:k,s} \\ &\quad + \sum_{k,s} \left[ c_3^0(\Gamma; A) \cos\left(\frac{k}{2}\right) a_{1:k,s}^\dagger a_{2:k,s} + \text{H.c.} \right], \end{aligned} \quad (3.5)$$

$$h^0(\Gamma; B) = \sum_{k,s} \left[ c_1^0(\Gamma; B) \sin\left(\frac{k}{2}\right) a_{1:k,s}^\dagger a_{2:k,s} + \text{H.c.} \right], \quad (3.6)$$

(3.1) because all the irreducible representations of  $\mathbf{C}_2$  are of one dimension.  $\mathcal{H}_{\text{HF}}$  is decomposed into spatial-symmetry-definite components as

$$\mathcal{H}_{\text{HF}} = \sum_{K=\Gamma,X} \sum_{D=A,B} \sum_{\lambda=0,z} h^\lambda(K; D), \quad (3.4)$$

where  $h^\lambda(K; D)$  is the irreducible basis Hamiltonian which belongs to the  $D$  representation at point  $K$  and is specified as

$$h^0(X; A) = \sum_{k,s} c_1^0(X; A) a_{1:k+\pi,s}^\dagger a_{1:k,s} + \sum_{k,s} \left[ c_2^0(X; A) \cos\left(\frac{k}{2}\right) a_{1:k+\pi,s}^\dagger a_{2:k,s} + \text{H.c.} \right], \quad (3.7)$$

$$h^0(X; B) = \sum_{k,s} c_1^0(X; B) a_{2:k+\pi,s}^\dagger a_{2:k,s} + \sum_{k,s} \left[ c_2^0(X; B) \sin\left(\frac{k}{2}\right) a_{1:k+\pi,s}^\dagger a_{2:k,s} + \text{H.c.} \right], \quad (3.8)$$

$$h^z(\Gamma; A) = \sum_{k,s,s'} c_1^z(\Gamma; A) a_{1:k,s}^\dagger a_{1:k,s'} \sigma_{ss'}^z + \sum_{k,s,s'} c_2^z(\Gamma; A) a_{2:k,s}^\dagger a_{2:k,s'} \sigma_{ss'}^z + \sum_{k,s,s'} \left[ c_3^z(\Gamma; A) \cos\left(\frac{k}{2}\right) a_{1:k,s}^\dagger a_{2:k,s'} \sigma_{ss'}^z + \text{H.c.} \right], \quad (3.9)$$

$$h^z(\Gamma; B) = \sum_{k,s,s'} \left[ c_1^z(\Gamma; B) \sin\left(\frac{k}{2}\right) a_{1:k,s}^\dagger a_{2:k,s'} \sigma_{ss'}^z + \text{H.c.} \right], \quad (3.10)$$

$$h^z(X; A) = \sum_{k,s,s'} c_1^z(X; A) a_{1:k+\pi,s}^\dagger a_{1:k,s'} \sigma_{ss'}^z + \sum_{k,s,s'} \left[ c_2^z(X; A) \cos\left(\frac{k}{2}\right) a_{1:k+\pi,s}^\dagger a_{2:k,s'} \sigma_{ss'}^z + \text{H.c.} \right], \quad (3.11)$$

$$h^z(X; B) = \sum_{k,s,s'} c_1^z(X; B) a_{2:k+\pi,s}^\dagger a_{2:k,s'} + \sum_{k,s,s'} \left[ c_2^z(X; B) \sin\left(\frac{k}{2}\right) a_{1:k+\pi,s}^\dagger a_{2:k,s'} \sigma_{ss'}^z + \text{H.c.} \right], \quad (3.12)$$

with

$$c_1^0(\Gamma; A) = \varepsilon_M + \frac{U_M}{L} \sum_k \rho_{11}^0(\Gamma; k) + \frac{4V}{L} \sum_k \rho_{22}^0(\Gamma; k),$$

$$c_2^0(\Gamma; A) = \varepsilon_X + \frac{U_X}{L} \sum_k \rho_{22}^0(\Gamma; k) + \frac{4V}{L} \sum_k \rho_{11}^0(\Gamma; k),$$

$$c_3^0(\Gamma; A) = -2t_0 - \frac{2V}{L} \sum_k \cos\left(\frac{k}{2}\right) \rho_{12}^0(\Gamma; k), \quad (3.13)$$

$$c_1^0(\Gamma; B) = \frac{2i\alpha}{\sqrt{L}} u_0 - \frac{2V}{L} \sum_k \sin\left(\frac{k}{2}\right) \rho_{12}^0(\Gamma; k), \quad (3.14)$$

$$c_1^0(X; A) = \frac{2i\beta}{\sqrt{L}} u_\pi + \frac{U_M}{L} \sum_k \rho_{11}^0(\Gamma; k),$$

$$c_2^0(X; A) = -\frac{2i\alpha}{\sqrt{L}} u_\pi + \frac{2V}{L} \sum_k \cos\left(\frac{k}{2}\right) \rho_{12}^0(X; k + \pi), \quad (3.15)$$

$$c_1^0(X; B) = -\frac{U_X}{L} \sum_k \rho_{22}^0(X; k + \pi),$$

$$c_2^0(X; B) = \frac{2V}{L} \sum_k \sin\left(\frac{k}{2}\right) \rho_{12}^0(X; k + \pi), \quad (3.16)$$

$$c_1^z(\Gamma; A) = -\frac{U_M}{L} \sum_k \rho_{11}^z(\Gamma; k),$$

$$c_2^z(\Gamma; A) = -\frac{U_X}{L} \sum_k \rho_{22}^z(\Gamma; k),$$

$$c_3^z(\Gamma; A) = -\frac{2V}{L} \sum_k \cos\left(\frac{k}{2}\right) \rho_{12}^z(\Gamma; k), \quad (3.17)$$

$$c_1^z(\Gamma; B) = -\frac{2V}{L} \sum_k \sin\left(\frac{k}{2}\right) \rho_{12}^z(\Gamma; k), \quad (3.18)$$

$$c_1^z(X; A) = -\frac{U_M}{L} \sum_k \rho_{11}^z(X; k + \pi),$$

$$c_2^z(X; A) = \frac{2V}{L} \sum_k \cos\left(\frac{k}{2}\right) \rho_{12}^z(X; k + \pi), \quad (3.19)$$

$$c_1^z(X; B) = \frac{U_X}{L} \sum_k \rho_{22}^z(X; k + \pi),$$

$$c_2^z(X; B) = \frac{2V}{L} \sum_k \sin\left(\frac{k}{2}\right) \rho_{12}^z(X; k + \pi). \quad (3.20)$$

We list in Table I the thus-obtained HF Hamiltonians of broken symmetry, where their invariance groups are also displayed. Once a broken-symmetry Hamiltonian is given, its invariance group is defined in such a way that any symmetry operation in the group keeps the Hamiltonian unchanged. Keeping in mind that the density matrices characteristic of the Hamiltonian given should also be invariant for its invariance group, we can completely determine qualitative properties of the solution [15,16].

Let us introduce relevant order parameters. The local charge density on site  $i$  at the  $n$ th unit cell is defined as

$$d_{i:n} \equiv \sum_s \langle a_{i:n,s}^\dagger a_{i:n,s} \rangle_{\text{HF}}, \quad (3.21)$$

the local spin density on site  $i$  at the  $n$ th unit cell as

$$s_{i:n}^z \equiv \frac{1}{2} \sum_{s,s'} \langle a_{i:n,s}^\dagger a_{i:n,s'} \rangle_{\text{HF}} \sigma_{ss'}^z, \quad (3.22)$$

the complex bond order between site  $i$  at the  $n$ th unit cell and site  $j$  at the  $m$ th unit cell as

$$p_{i:n;j:m} \equiv \sum_s \langle a_{i:n,s}^\dagger a_{j:m,s} \rangle_{\text{HF}}, \quad (3.23)$$

and the complex spin bond order between site  $i$  at the  $n$ th unit cell and site  $j$  at the  $m$ th unit cell as

$$t_{i:n;j:m}^z \equiv \frac{1}{2} \sum_{s,s'} \langle a_{i:n,s}^\dagger a_{j:m,s'} \rangle_{\text{HF}} \sigma_{ss'}^z. \quad (3.24)$$

The halogen-atom displacements  $u_n$  are self-consistently determined so as to minimize the HF energy  $E_{\text{HF}} \equiv \langle \mathcal{H} \rangle_{\text{HF}}$ . Now we are ready to classify and characterize all the possible solutions. We are convinced in the following that any order parameter unspecified is zero and  $\bar{\rho}_{ij}^\lambda(K; k)$  and  $\tilde{\rho}_{ij}^\lambda(K; k)$  denote the real and imaginary parts of  $\rho_{ij}^\lambda(K; k)$ , respectively. The solutions obtained are schematically shown in Fig. 1.

#### A. $\Gamma A \otimes \check{S}^0 \otimes \check{T}^0$

$$\begin{aligned} d_{1:n} &= \frac{2}{L} \sum_k \bar{\rho}_{11}^0(\Gamma; k), & d_{2:n} &= \frac{2}{L} \sum_k \bar{\rho}_{22}^0(\Gamma; k), \\ p_{1:n;2:n} &= p_{1:n;2:n-1} = \frac{2}{L} \sum_k \cos\left(\frac{k}{2}\right) \bar{\rho}_{21}^0(\Gamma; k). \end{aligned} \quad (3.25)$$

This phase (Fig. 1a) possesses the full symmetry (2.8) and is recognized as the paramagnetic state. We abbreviate the state as PM.

#### B. $\Gamma B \otimes \check{S}^0 \otimes \check{T}^0$

$$\begin{aligned} d_{1:n} &= \frac{2}{L} \sum_k \bar{\rho}_{11}^0(\Gamma; k), & d_{2:n} &= \frac{2}{L} \sum_k \bar{\rho}_{22}^0(\Gamma; k), \\ p_{1:n;2:n} &= \frac{2}{L} \sum_k \cos\left(\frac{k}{2}\right) \bar{\rho}_{21}^0(\Gamma; k) - \frac{2}{L} \sum_k \sin\left(\frac{k}{2}\right) \tilde{\rho}_{21}^0(\Gamma; k), \\ p_{1:n;2:n-1} &= \frac{2}{L} \sum_k \cos\left(\frac{k}{2}\right) \bar{\rho}_{21}^0(\Gamma; k) + \frac{2}{L} \sum_k \sin\left(\frac{k}{2}\right) \tilde{\rho}_{21}^0(\Gamma; k), \\ u_n &= \frac{8\alpha}{L} \sum_k \sin\left(\frac{k}{2}\right) \tilde{\rho}_{21}^0. \end{aligned} \quad (3.26)$$

This phase (Fig. 1b) is characterized by the alternating bond orders with the uniform lattice deformation. We abbreviate the state as BOW. Here is no alternation of on-site charge densities and the site-diagonal el-ph coupling  $\beta$  is irrelevant.

#### C. $X A \otimes \check{S}^0 \otimes \check{R}^0$

$$\begin{aligned} d_{1:n} &= \frac{2}{L} \sum_k \bar{\rho}_{11}^0(\Gamma; k) + \frac{2(-1)^n}{L} \sum_k \bar{\rho}_{11}^0(X; k), & d_{2:n} &= \frac{2}{L} \sum_k \bar{\rho}_{22}^0(\Gamma; k), \\ p_{1:n;2:n} &= p_{1:n;2:n-1} = \frac{2}{L} \sum_k \cos\left(\frac{k}{2}\right) \bar{\rho}_{21}^0(\Gamma; k) - \frac{2(-1)^n}{L} \sum_k \sin\left(\frac{k}{2}\right) \bar{\rho}_{21}^0(X; k), \\ u_n &= -\frac{4\beta(-1)^n}{L} \sum_k \bar{\rho}_{11}^0(X; k). \end{aligned} \quad (3.27)$$

This phase (Fig. 1c) is characterized by the alternating charge densities on the metal sites induced by the lattice dimerization. We abbreviate the state as M-CDW. While both site-diagonal ( $\beta$ ) and site-off-diagonal ( $\alpha$ ) el-ph interactions contribute to the energy stabilization of the state,  $\beta$  is much more relevant here.

**D.**  $XB \otimes \check{S}^0 \otimes \check{T}^0$

$$\begin{aligned}
d_{1:n} &= \frac{2}{L} \sum_k \bar{\rho}_{11}^0(\Gamma; k), \quad d_{2:n} = \frac{2}{L} \sum_k \bar{\rho}_{22}^0 + \frac{2(-1)^n}{L} \sum_k \bar{\rho}_{22}^0(X; k), \\
p_{1:n;2:n} &= \frac{2}{L} \sum_k \cos\left(\frac{k}{2}\right) \bar{\rho}_{21}^0(\Gamma; k) - \frac{2(-1)^n}{L} \sum_k \sin\left(\frac{k}{2}\right) \bar{\rho}_{21}^1(X; k), \\
p_{1:n;2:n-1} &= \frac{2}{L} \sum_k \cos\left(\frac{k}{2}\right) \bar{\rho}_{21}^0(\Gamma; k) + \frac{2(-1)^n}{L} \sum_k \sin\left(\frac{k}{2}\right) \bar{\rho}_{21}^1(X; k).
\end{aligned} \tag{3.28}$$

This phase (Fig. 1d) is characterized by the alternating charge densities on the halogen sites with a purely electronic bond order wave. We abbreviate the state as X-CDW.

**E.**  $\Gamma A \otimes \check{S}^1 \otimes \check{T}^1$

$$\begin{aligned}
d_{1:n} &= \frac{2}{L} \sum_k \bar{\rho}_{11}^0(\Gamma; k), \quad d_{2:n} = \frac{2}{L} \sum_k \bar{\rho}_{22}^0(\Gamma; k), \\
p_{1:n;2:n} &= p_{1:n;2:n-1} = \frac{2}{L} \sum_k \cos\left(\frac{k}{2}\right) \bar{\rho}_{21}^0(\Gamma; k), \\
s_{1:n}^z &= \frac{1}{L} \sum_k \bar{\rho}_{11}^z(\Gamma; k), \quad s_{2:n}^z = \frac{1}{L} \sum_k \bar{\rho}_{22}^z(\Gamma; k), \\
t_{1:n;2:n}^z &= t_{1:n;2:n-1}^z = \frac{1}{L} \sum_k \cos\left(\frac{k}{2}\right) \bar{\rho}_{21}^z(\Gamma; k).
\end{aligned} \tag{3.29}$$

This phase (Fig. 1e) is the ferromagnetism with the uniform spin bond orders. We abbreviate the state as FM. We note that not only the metal sites but also the halogen sites have spin densities.

**F.**  $\Gamma B \otimes \check{S}^1 \otimes \check{T}^1$

$$\begin{aligned}
d_{1:n} &= \frac{2}{L} \sum_k \bar{\rho}_{11}^0(\Gamma; k), \quad d_{2:n} = \frac{2}{L} \sum_k \bar{\rho}_{22}^0(\Gamma; k), \\
p_{1:n;2:n} &= p_{1:n;2:n-1} = \frac{2}{L} \sum_k \cos\left(\frac{k}{2}\right) \bar{\rho}_{21}^0(\Gamma; k), \\
t_{1:n;2:n}^z &= -t_{1:n;2:n-1}^z = -\frac{1}{L} \sum_k \sin\left(\frac{k}{2}\right) \bar{\rho}_{21}^z(\Gamma; k).
\end{aligned} \tag{3.30}$$

This phase (Fig. 1f) is characterized by the alternating spin bond orders. Both metal and halogen sites have no spin density. We abbreviate the state as SBOW.

**G.**  $XA \otimes \check{S}^1 \otimes \check{T}^1$

$$\begin{aligned}
d_{1:n} &= \frac{2}{L} \sum_k \bar{\rho}_{11}^0(\Gamma; k), \quad d_{2:n} = \frac{2}{L} \sum_k \bar{\rho}_{22}^0(\Gamma; k), \\
p_{1:n;2:n} &= p_{1:n;2:n-1} = \frac{2}{L} \sum_k \cos\left(\frac{k}{2}\right) \bar{\rho}_{21}^0(\Gamma; k), \\
s_{1:n}^z &= \frac{(-1)^n}{L} \sum_k \bar{\rho}_{11}^z(X; k), \quad s_{2:n}^z = 0, \\
t_{1:n;2:n}^z &= t_{1:n;2:n-1}^z = \frac{(-1)^n}{L} \sum_k \cos\left(\frac{k}{2}\right) \bar{\rho}_{21}^z(X; k).
\end{aligned} \tag{3.31}$$

This phase (Fig. 1g) is characterized by the alternating spin densities on the metal sites with the alternating spin bond orders. We abbreviate the state as M-SDW.

### H. $XB \otimes \check{S}^1 \otimes \check{T}^1$

$$\begin{aligned}
d_{1:n} &= \frac{2}{L} \sum_k \bar{\rho}_{11}^0(\Gamma; k), \quad d_{2:n} = \frac{2}{L} \sum_k \bar{\rho}_{22}^0(\Gamma; k), \\
p_{1:n;2:n} &= p_{1:n;2:n-1} = \frac{2}{L} \sum_k \cos\left(\frac{k}{2}\right) \bar{\rho}_{21}^0(\Gamma; k), \\
s_{1:n}^z &= 0, \quad s_{2:n}^z = \frac{(-1)^n}{L} \sum_k \tilde{\rho}_{22}^z(X; k), \\
t_{1:n;2:n}^z &= -t_{1:n;2:n-1}^z = -\frac{(-1)^n}{L} \sum_k \sin\left(\frac{k}{2}\right) \tilde{\rho}_{21}^z(X; k).
\end{aligned} \tag{3.32}$$

This phase (Fig. 1h) is characterized by the alternating spin densities on the halogen sites with the alternating spin bond orders. We abbreviate the state as X-SDW.

So-far-synthesized MX compounds exhibit ground states of M-CDW or M-SDW type. We will later visualize the competition [21] between them, which is essentially described by the two parameters,  $\beta$  and  $U_M$ . The ferroelectric ground states [10,22] of mixed-stack CT compounds are recognized as BOW, where  $\alpha$  is most relevant. The ferromagnetic ground states [23] of organic radical crystals may qualitatively be identified with FM, where strong on-site Coulomb interactions are essential. Thus it is implied that M-CDW and M-SDW are most stabilized at 3/4 band filling, whereas BOW and FM around half band filling. Generally,  $\Gamma$ - and  $X$ -phases are, respectively, more and less stabilized as the system moves away from 3/4 band filling. Our approach shows that only the nonmagnetic solutions can be accompanied by lattice deformation. Further harvests may be a few novel density-wave states, X-CDW, SBOW, and X-SDW. We note that M-CDW is stabilized in a lattice dimerized, whereas no lattice distortion accompanies X-CDW. It is also worth while noting that the three-band model for the  $\text{CuO}_2$  planes in high-temperature superconductors also has a solution of the same type as X-SDW, namely, the SDW on the oxygen sites [4,5,24]. Assuming that doped holes should predominantly be of halogen character on the analogy of the model in two dimension [25], hole doping may cause the frustration of an antiferromagnetic spin alignment on the metal sites and therefore lead to the collapse of M-SDW.

## IV. NUMERICAL CALCULATION AND DISCUSSION

Plenty of parameters may potentially bring rich ground-state phase diagrams. In order to have a general view of the model, we here restrict relevant parameters to the difference between the M- and X-atom on-site affinities,  $\varepsilon_0 \equiv \varepsilon_M - \varepsilon_X$ , the on-site Coulomb interactions,  $U_M$  and  $U_X$ , and band filling. The HF energy is calculated in the thermodynamic limit.

We show in Fig. 2 phase diagrams at 3/4 band filling, where  $q = \pi$  states are predominantly stabilized.

As far as magnetic instabilities are concerned, the phase diagram at  $\varepsilon_0 = 0$  is almost symmetric under the exchange of  $U_M$  and  $U_X$ . This is because magnetic phases are accompanied by no lattice deformation. It is not the case with nonmagnetic instabilities. Here the metal-atom displacements are assumed to be much smaller than the halogen-atom ones and thus negligible. Therefore, X-CDW is strongly suppressed and M-CDW is predominantly stabilized due to the el-ph coupling  $\beta$ . With the increase of  $\varepsilon_0$ , density waves on the halogen sites are generally reduced and single-band models come to be justified. The phase boundary between M-SDW and X-SDW is roughly given by  $U_X - U_M = 1.8\varepsilon_0$ . In comparison with MX compounds with  $M = \text{Pt}$  and  $M = \text{Pd}$  whose ground states are M-CDW, Ni complexes relatively have a small  $\varepsilon_0$  and a large  $U_M$  [26] and thus exhibit M-SDW ground states. In order to realize X-SDW ground states, a small enough  $\varepsilon_0$  and a large enough  $U_X$  are necessary.

We show in Fig. 3 phase diagrams at half band filling, where  $q = 0$  states are relatively stabilized. The off-site el-ph coupling  $\alpha$  stabilizes BOW, whereas the off-site Coulomb interaction  $V$  is unfavorable to that. The increase of  $V$  generally turns BOW into PM. All the present findings are consistent with the observations [10,22] of mixed-stack CT compounds. Here we could not have a quantitative argument on FM. The present approach never goes beyond the Stoner's theory [27] and thus concludes that once the system deviates from 3/4 band filling, FM can necessarily appear with large enough  $U_M$  and  $U_X$ . It is, however, well-known that multiscattering effects [28] qualitatively correct this scenario. The ferromagnetism in multiband models [29–31] is a subject of great interest in itself and should be investigated taking account of intra-atomic exchange interactions, which favors a ferromagnetic spin alignment.

Finally we briefly observe the doping dependences of the states appearing in the phase diagrams. We define macroscopic order parameters as

$$O_{\text{M-CDW}} = \frac{1}{L} \sum_n (-1)^n d_{1:n}, \tag{4.1}$$

$$O_{\text{M-SDW}} = \frac{1}{L} \sum_n (-1)^n s_{1:n}^z, \quad (4.2)$$

$$O_{\text{X-SDW}} = \frac{1}{L} \sum_n (-1)^n s_{2:n}^z, \quad (4.3)$$

$$O_{\text{BOW}} = \frac{1}{2L} \sum_n (p_{1:n;2:n-1} - p_{1:n;2:n}), \quad (4.4)$$

$$O_{\text{FM}}^{\text{M}} = \frac{1}{L} \sum_n s_{1:n}^z, \quad O_{\text{FM}}^{\text{X}} = \frac{1}{L} \sum_n s_{2:n}^z, \quad (4.5)$$

and show them as functions of band filling in Table II, where the last digit of each estimate may contain a slight numerical uncertainty. Now we explicitly find that M-CDW, M-SDW, and X-SDW are most stabilized at 3/4 band filling, while BOW and FM at half band filling. Concerning FM we note that  $O_{\text{FM}}^{\text{M}}$  and  $O_{\text{FM}}^{\text{X}}$  have opposite signs, which means spins on the metal and halogen sites are antiparallel to each other (Fig. 1e). When we move away from half band filling, electrons are preferably doped into the halogen sites, whereas holes into the metal sites. Further numerical investigation will be presented elsewhere.

While X-CDW and SBOW do not appear in the ground-state phase diagrams shown here, we expect them in a more extensive numerical investigation. Even if the states are scarcely stabilized into a ground state, they can still be relevant in the ground-state correlations. We note, for example, that low-lying solitonic excitations in a SDW ground state induce SBOW domains around their centers [32]. Besides the obtained novel density-wave states themselves, we stress the wide applicability of the present approach. Although the approach is feasible and even more enlightening in higher dimensions [4,5], fascinating materials such as halogen-bridged binuclear complexes [33] and DCNQI-Cu systems exhibiting a three-fold superlattice structure [34] stimulate us to further explorations in one dimension, where the problem of competing ground states is really fruitful. Even if a model treated is of one dimension, its complicated unit-cell structure and various el-ph interactions may conceal some of instabilities of importance from our naive guess. Our approach never fails to reveal all the possible broken-symmetry phases. We hope that the present argument will motivate further chemical, as well as theoretical, explorations in low-dimensional el-ph systems.

## ACKNOWLEDGMENTS

It is a pleasure to thank M. Ozaki for his useful discussion. The author is furthermore grateful to Y. Nogami and H. Okamoto for their helpful comments on materials of current interest. A part of the numerical calculation was done using the facility of the supercomputer center, Institute for Solid State Physics, University of Tokyo. This work is supported in part by the Japanese Ministry of Education, Science, and Culture through the

Grant-in-Aid 09740286 and by the Okayama Foundation for Science and Technology.

- 
- [1] J. T. Gammel, I. Batistić, A. R. Bishop, E. Y. Loh, Jr., and S. Marianer, *Physica B* **163** (1990) 458.
  - [2] D. Baeriswyl and A. R. Bishop, *Phys. Scr.* **T19** (1987) 239; *J. Phys. C* **21** (1988) 339.
  - [3] K. Nasu, *J. Phys. Soc. Jpn.* **52** (1983) 3865; **53** (1984) 302; **53** (1984) 427.
  - [4] S. Yamamoto and M. Ozaki, *Solid State Commun.* **83** (1992) 329; **83** (1992) 335.
  - [5] S. Yamamoto and M. Ozaki, in *Group Theoretical Methods in Physics*, edited by A. Arima, T. Eguchi, and N. Nakanishi (World Scientific, Singapore, 1995), p. 499.
  - [6] J. T. Gammel, A. Saxena, I. Batistić, A. R. Bishop, and S. R. Phillpot, *Phys. Rev. B* **45** (1992) 6408; S. W. Weber-Milbrodt, J. T. Gammel, A. R. Bishop, and E. Y. Loh, Jr., *ibid.* **45** (1992) 6435.
  - [7] K. Yonemitsu, A. R. Bishop, and J. Lorenzana, *Phys. Rev. B* **47** (1993) 8065.
  - [8] A. R. Bishop and J. T. Gammel, *Synth. Met.* **29** (1989) F151; I. Batistić, J. T. Gammel, and A. R. Bishop, *Phys. Rev. B* **44** (1991) 13228.
  - [9] J. T. Gammel, K. Yonemitsu, A. Saxena, A. R. Bishop, and H. Röder, *Synth. Met.* **55-57** (1993) 3377; H. Röder, A. R. Bishop, and J. T. Gammel, *Phys. Rev. Lett.* **70** (1993) 3498.
  - [10] J. B. Torrance, J. E. Vazquez, J. J. Mayerle, and V. Y. Lee, *Phys. Rev. Lett.* **46** (1981) 253; J. B. Torrance, A. Girlando, J. J. Mayerle, J. I. Crowley, V. Y. Lee, P. Batail, and S. J. LaPlaca, *Phys. Rev. Lett.* **47** (1981) 1747.
  - [11] N. Iwasawa, S. Shinozaki, G. Saito, K. Oshima, T. Mori, and H. Inokuchi, *Chem. Lett.* (1988) 215.
  - [12] H. J. Keller, in *Extended Linear Chain Compounds*, edited by J. S. Miller (Plenum, New York, 1983), Vol. 1, P. 357.
  - [13] H. Toftlund and O. Simonsen, *Inorg. Chem.* **23** (1984) 4261.
  - [14] K. Toriumi, Y. Wada, T. Mitani, S. Bandow, M. Yamashita, and Y. Fujii, *J. Am. Chem. Soc.* **111** (1989) 2341.
  - [15] M. Ozaki, *Int. J. Quantum Chem.* **42** (1992) 55.
  - [16] S. Yamamoto and M. Ozaki, *Int. J. Quantum Chem.* **44** (1992) 949.
  - [17] M. Ozaki, *Prog. Theor. Phys.* **67** (1982) 83; **67** (1982) 415.
  - [18] M. Ozaki, *J. Math. Phys.* **26**, 1514 (1985); **26** (1985) 1521.
  - [19] C. J. Bradley and C. P. Cracknell, *The Mathematical Theory of Symmetry in Solids* (Clarendon, Oxford, 1972).
  - [20] I. Affleck and J. B. Marston, *Phys. Rev. B* **37** (1988) 3774.
  - [21] K. Nasu and Y. Toyozawa, *J. Phys. Soc. Jpn.* **51** (1982) 2098; **51** (1982) 3111.



- [22] Y. Tokura, S. Koshihara, Y. Iwasa, H. Okamoto, T. Komatsu, T. Koda, N. Iwasawa, and G. Saito, *Phys. Rev. Lett.* **63** (1989) 2405.
- [23] M. Kinoshita, P. Turek, M. Tamura, K. Nozawa, D. Shiomi, Y. Nakazawa, M. Ishikawa, M. Takahashi, K. Awaga, T. Inabe, and Y. Maruyama, *Chem. Lett.* (1991) 1225; M. Takahashi, P. Turek, Y. Nakazawa, M. Tamura, K. Nozawa, D. Shiomi, M. Ishikawa, and M. Kinoshita, *Phys. Rev. Lett.* **67** (1991) 746.
- [24] M. Weinert and G. W. Fernando, *Phys. Rev. B* **39** (1989) 835.
- [25] J. Dutka and A. M. Oleś, *Phys. Rev. B* **42** (1990) 105; and references therein.
- [26] H. Okamoto, Y. Shimada, Y. Oka, A. Chainani, T. Takahashi, H. Kitagawa, T. Mitani, K. Toriumi, K. Inoue, T. Manabe, and M. Yamashita, *Phys. Rev. B* **54** (1996) 8438.
- [27] E. C. Stoner, *Rep. Prog. Phys.* **11** (1946) 43.
- [28] J. Kanamori, *Prog. Theor. Phys.* **30** (1963) 275.
- [29] H. Shiba, *Prog. Theor. Phys.* **48** (1972) 2171.
- [30] Y. Nagaoka, *Prog. Theor. Phys.* **52** (1974) 1716.
- [31] K. Kusakabe and H. Aoki, *Physica B* **194-196** (1994) 217.
- [32] Y. Shimoi and H. Fukutome, *Solid State Commun.* **82** (1992) 407.
- [33] T. Mitani, T. Sonoyama, M. Yamamoto, H. Kitagawa, and M. Fukawa, unpublished.
- [34] R. Kato, H. Kobayashi, and A. Kobayashi, *J. Am. Chem. Soc.* **111** (1989) 5224.

FIG. 1. Schematic representation of possible density-wave states, where the variety of circles and segments qualitatively represents the variation of local charge densities and bond orders, respectively, whereas the signs  $\pm$  in circles and strips describe the alternation of local spin densities and spin bond orders, respectively. Circles shifted from their equidistant location qualitatively represent X-atom displacements. Identifying the present system, for example, with halogen-bridged metal complexes, each phase is characterized as follows: (a) Paramagnetism; (b) Electron-phonon bond order wave; (c) Metal charge density wave accompanied by an electron-phonon bond order wave; (d) Halogen charge density wave accompanied by a purely electronic bond order wave; (e) Ferromagnetism with uniform spin bond orders; (f) Spin bond order wave; (g) Metal spin density wave accompanied by a spin bond order wave; (h) Halogen spin density wave accompanied by a spin bond order wave.

FIG. 2. Ground-state phase diagrams at various values of  $\varepsilon_0$ : (a)  $\varepsilon_0/t_0 = 0.0$ ; (b)  $\varepsilon_0/t_0 = 1.0$ ; (c)  $\varepsilon_0/t_0 = 2.0$ . Here the following parametrization is common to all:  $V/t_0 = 1.0$ ,  $\alpha/(Kt_0)^{1/2} = 0.1$ ,  $\beta/(Kt_0)^{1/2} = 1.0$ , and  $3/4$  band filling.

FIG. 3. Ground-state phase diagrams at various values of el-ph coupling constants: (a)  $\alpha/(Kt_0)^{1/2} = 0.6$ ,  $\beta/(Kt_0)^{1/2} = 1.0$ ; (b)  $\alpha/(Kt_0)^{1/2} = 0.8$ ,  $\beta/(Kt_0)^{1/2} = 0.1$ . Here the following parametrization is common to all:  $\varepsilon_0/t_0 = 3.0$ ,  $V/t_0 = 1.0$ , and half band filling.

TABLE I. Hartree-Fock broken-symmetry Hamiltonians, their invariance groups, and consequent density-wave states.

Representation	Hamiltonian	Invariance group	State
$\Gamma A \otimes \check{S}^0 \otimes \check{T}^0$	$h^0(\Gamma; A)$	$\mathbf{L}_1 \mathbf{C}_2 \mathbf{ST}$	PM
$\Gamma B \otimes \check{S}^0 \otimes \check{T}^0$	$h^0(\Gamma; A) + h^0(\Gamma; B)$	$\mathbf{L}_1 \mathbf{ST}$	BOW
$XA \otimes \check{S}^0 \otimes \check{T}^0$	$h^0(\Gamma; A) + h^0(X; A)$	$\mathbf{L}_2 \mathbf{C}_2 \mathbf{ST}$	M-CDW
$XB \otimes \check{S}^0 \otimes \check{T}^0$	$h^0(\Gamma; A) + h^0(X; B)$	$(1 + l_1 C_2) \mathbf{L}_2 \mathbf{ST}$	X-CDW
$\Gamma A \otimes \check{S}^1 \otimes \check{T}^1$	$h^0(\Gamma; A) + h^z(\Gamma; A)$	$\mathbf{L}_1 \mathbf{C}_2 \mathbf{A}(\mathbf{e}_z) \mathbf{M}(\mathbf{e}_\parallel)$	FM
$\Gamma B \otimes \check{S}^1 \otimes \check{T}^1$	$h^0(\Gamma; A) + h^z(\Gamma; B)$	$(1 + C_2 u(\mathbf{e}_\parallel, \pi)) \mathbf{L}_1 \mathbf{A}(\mathbf{e}_z) \mathbf{M}(\mathbf{e}_\parallel)$	SBOW
$XA \otimes \check{S}^1 \otimes \check{T}^1$	$h^0(\Gamma; A) + h^z(X; A)$	$(1 + l_1 u(\mathbf{e}_\parallel, \pi)) \mathbf{L}_2 \mathbf{C}_2 \mathbf{A}(\mathbf{e}_z) \mathbf{M}(\mathbf{e}_\parallel)$	M-SDW
$XB \otimes \check{S}^1 \otimes \check{T}^1$	$h^0(\Gamma; A) + h^z(X; B)$	$(1 + l_1 C_2)(1 + l_1 u(\mathbf{e}_\parallel, \pi)) \mathbf{L}_2 \mathbf{A}(\mathbf{e}_z) \mathbf{M}(\mathbf{e}_\parallel)$	X-SDW

<sup>a)</sup>  $\mathbf{L}_1$  is the translation group whose basis vector is the unit-cell translation  $l_1$ .

<sup>b)</sup>  $\mathbf{L}_2$  is the translation group whose basis vector is the double-unit-cell translation.

<sup>c)</sup>  $\mathbf{A}(\mathbf{e}_z) = \{u(\mathbf{e}_z, \theta) | 0 \leq \theta \leq 4\pi\}$  with the axis  $\mathbf{e}_z$  along the  $z$  direction.

<sup>d)</sup>  $\mathbf{M}(\mathbf{e}_\parallel) = \{E, tu(\mathbf{e}_\parallel, \pi)\}$  with the axis  $\mathbf{e}_\parallel$  along the chain direction.

TABLE II. Order parameters as functions of band filling.

Band filling	$O_{\text{M-CDW}}$	$O_{\text{M-SDW}}$	$O_{\text{X-SDW}}$
3.2/4.0	0.64977	0.32626	0.23942
3.1/4.0	0.74603	0.37371	0.28664
3.0/4.0	0.84207	0.42111	0.33321
2.9/4.0	0.78778	0.40047	0.32808
2.8/4.0	0.72453	0.37621	0.32137
Band filling	$O_{\text{BOW}}$	$O_{\text{FM}}^{\text{M}}$	$O_{\text{FM}}^{\text{X}}$
2.2/4.0	0.32294	0.42921	-0.32921
2.1/4.0	0.46682	0.43536	-0.38536
2.0/4.0	0.47283	0.44118	-0.44118
1.9/4.0	0.47147	0.38536	-0.43536
1.8/4.0	0.46954	0.32921	-0.42921

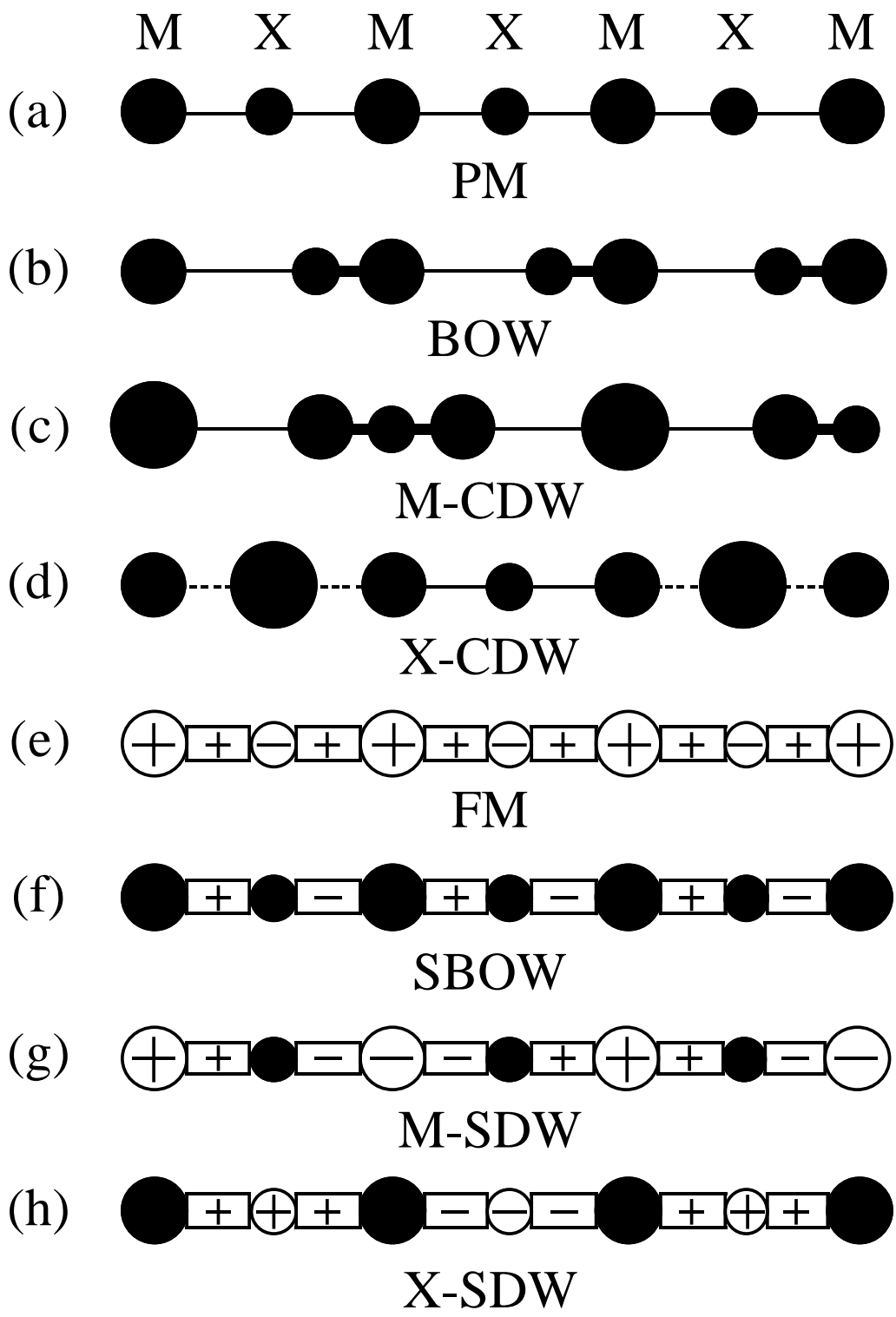


Fig.1 S. Yamamoto

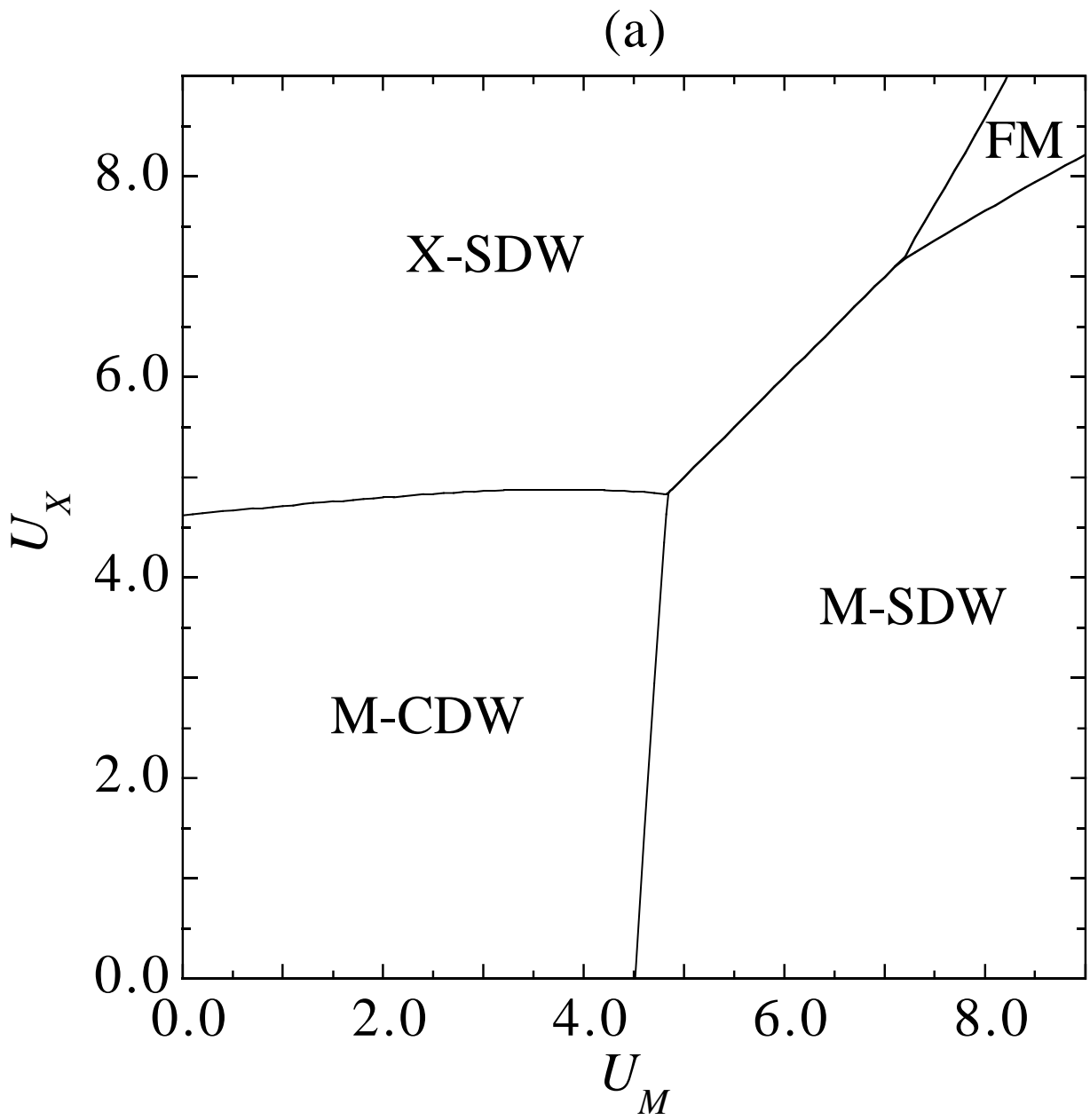


Fig.2(a) S. Yamamoto

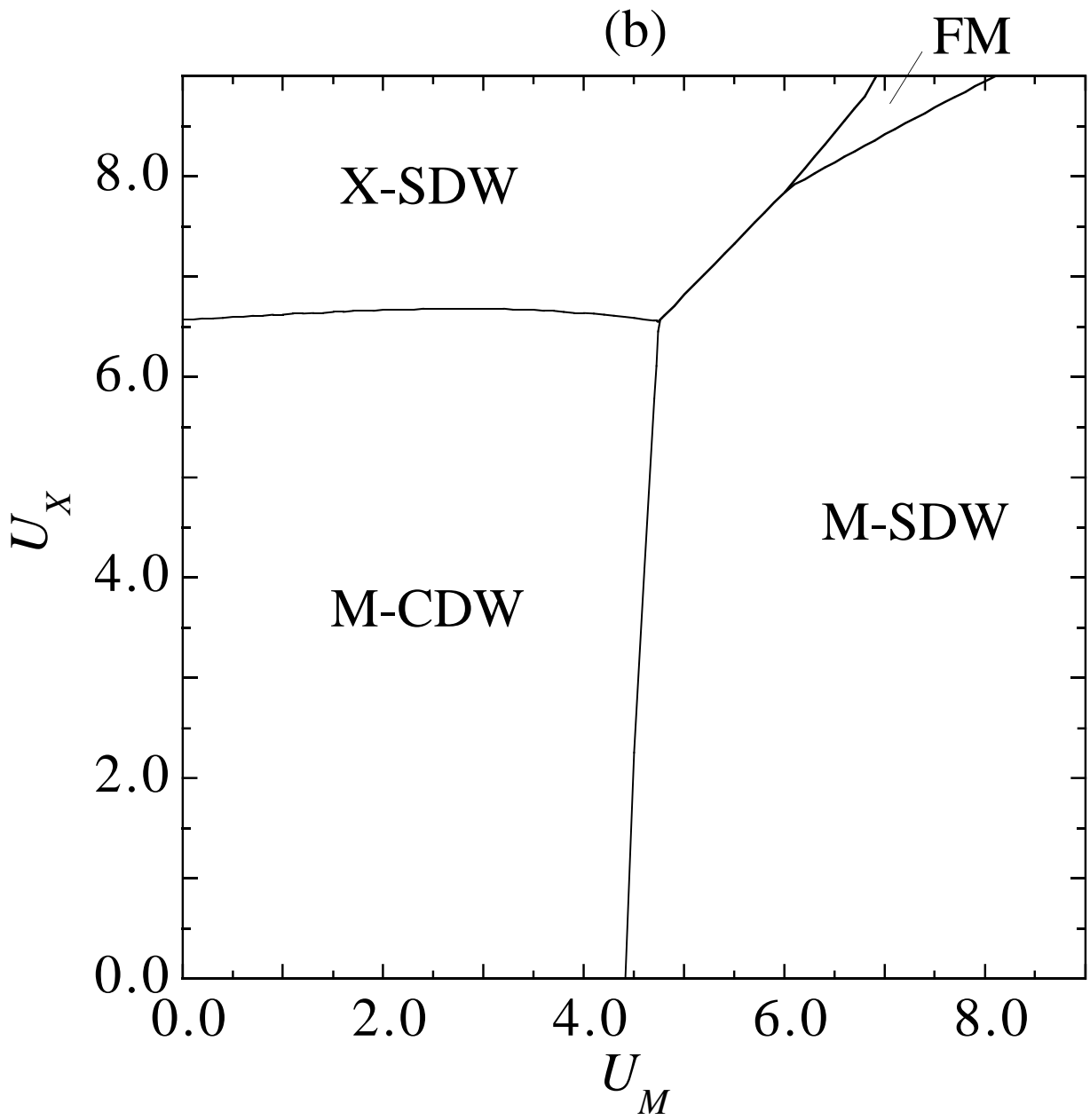


Fig.2 (b)

S. Yamamoto

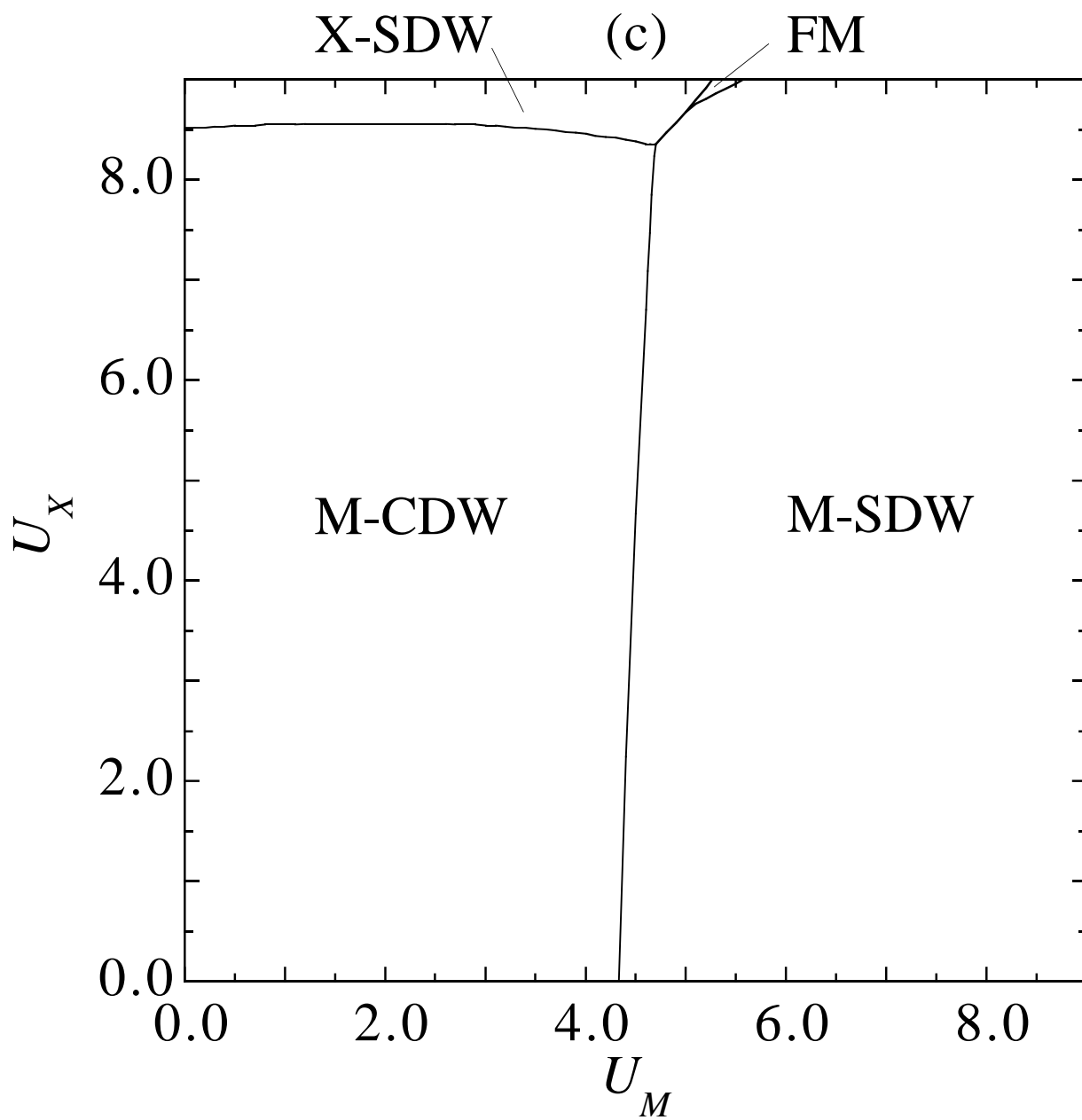


Fig.2(c) S. Yamamoto

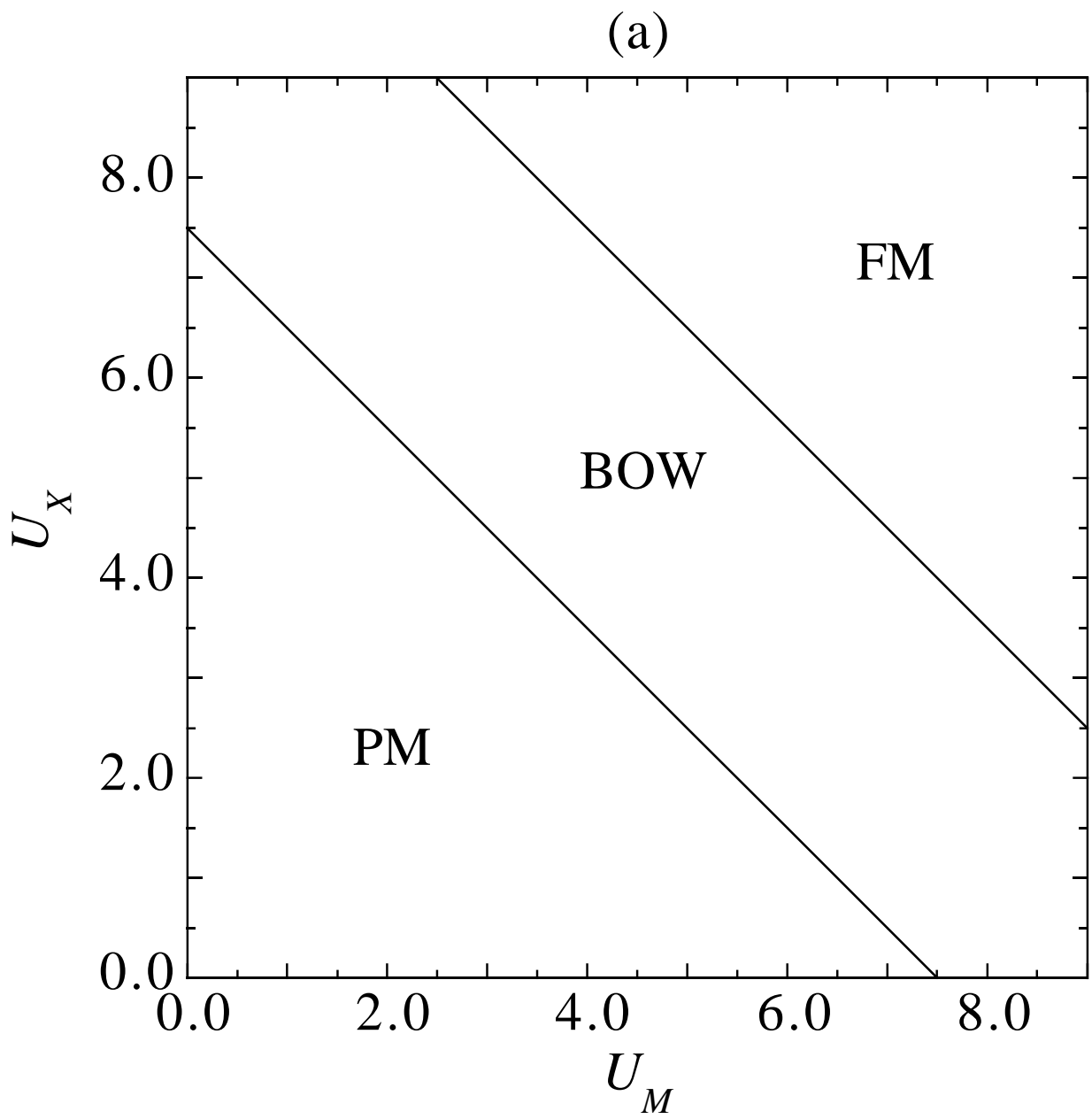


Fig.3(a) S. Yamamoto

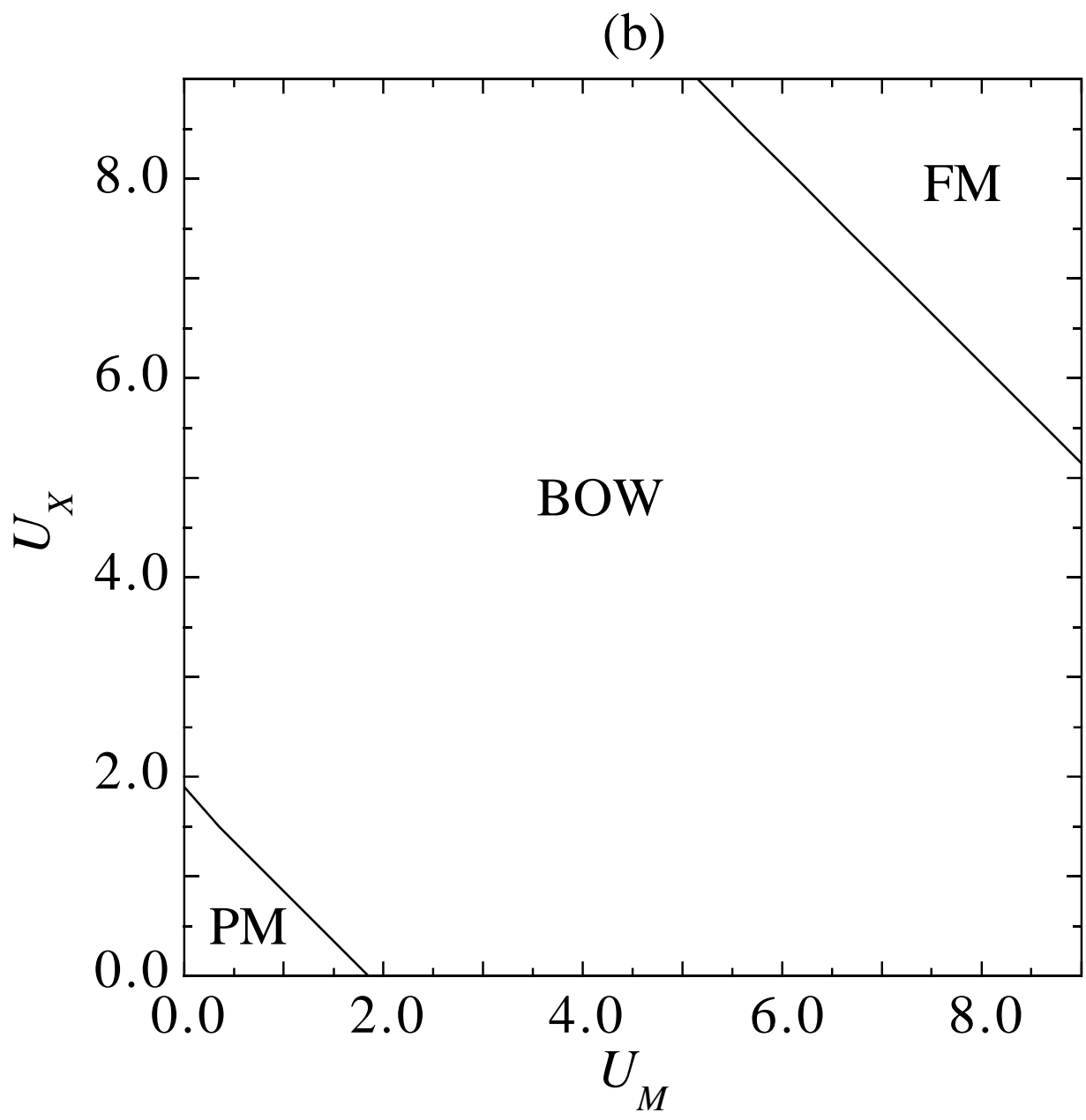


Fig.3(b) S. Yamamoto